EASR

Engineering and Applied Science Research

https://www.tci-thaijo.org/index.php/easr/index

Published by the Faculty of Engineering, Khon Kaen University, Thailand

Chitosan beads with *Calamondin* essential oil: Antioxidant, antimicrobial, physical, and structural properties

Le Pham Tan Quoc*, Tran Ho Anh Duy, Trinh Nhat Sinh and Lam Bach Bao Phuong

Institute of Biotechnology and Food Technology, Industrial University of Ho Chi Minh City, Ho Chi Minh City, Vietnam

Received 26 March 2025
Revised 31 July 2025
Accepted 5 August 2025

Abstract

Chitosan, a biopolymer renowned for its biodegradability and antimicrobial properties, is frequently enhanced with essential oils (EOs) to improve functionality. This study investigated the impact of incorporating calamondin EO (CmEO) into chitosan beads on their physicochemical properties, antioxidant activity, antibacterial efficacy, and structural characteristics. The incorporation of CmEO improved the sphericity of the beads, ranging from 68.20% to 87.59%, and produced 177–263 beads per 10 mL of solution, depending on the formulation. The addition of CmEO to chitosan beads significantly boosted antioxidant activity, with the highest concentration exhibiting radical scavenging activity of 77.96%. Antibacterial assays revealed that the chitosan beads with CmEO could inhibit the growth of *Escherichia coli*, *Bacillus cereus*, *Salmonella enteritidis*, and *Staphylococcus aureus*. Structural analysis shows significant changes on the bead surface corresponding to changes in CmEO concentration. These findings highlight the potential of chitosan-based materials enriched with EOs for sustainable food preservation.

Keywords: Chitosan beads, Antimicrobial activity, Antioxidant capacity, Physical properties, Structure

1. Introduction

In recent years, the utilization of biodegradable materials for food preservation has garnered significant attention due to escalating environmental concerns and the demand for sustainable alternatives to synthetic packaging [1]. Chitosan, a biopolymer derived from chitin, has been extensively studied for its biocompatibility, biodegradability, and remarkable antimicrobial properties. Its ability to form beads not only facilitates controlled active ingredient release, but also enhances antimicrobial efficacy, thereby amplifying its application potential in food preservation [2].

Essential oils (EOs) extracted from citrus fruits have demonstrated potent antioxidant and antimicrobial activities, rendering them promising candidates for integration into chitosan-based systems. Perdones et al. [3] examined the impact of chitosan coatings incorporating lemon EO for strawberry preservation and reported notable efficacy in extending shelf life and maintaining food quality. Junca et al. [4] incorporated *Thymus capitatus* EO into chitosan beads and observed enhanced antioxidant activity. Fourier-transform infrared (FTIR) spectroscopy showed stronger molecular interactions, with intensified vibration bands and reduced peak intensity, while X-ray diffraction (XRD) analysis revealed broadened peaks around 20°, indicating decreased crystallinity. These results highlight the potential of EO-loaded chitosan beads to improve both bioactivity and structural functionality for food preservation.

Calamondin (*Citrus microcarpa*) EO (CmEO) stands out due to its rich composition of bioactive compounds, particularly flavonoids and terpenes, which possess robust antimicrobial and antioxidant properties [5]. This study aimed to evaluate the physicochemical properties, antioxidant activity, antibacterial efficacy, and structural characteristics of chitosan beads containing varying concentrations of CmEO (CB-EO). While chitosan-based films and coatings containing EOs have been widely studied, there has been limited research on bead-based systems. The combination of chitosan beads with CmEO offers a novel approach for developing natural preservative carriers. This combination is hypothesized to enhance the functional attributes of the material, offering an effective and environmentally benign solution for food preservation. This work provides a new perspective on the formulation and characterization of EO-loaded biopolymer beads, contributing to the advancement of biodegradable and functional food packaging systems.

2. Materials and methods

2.1 Materials

Chitosan, with a deacetylation degree of ≥85%, was supplied by Thien Viet Company. CmEO was extracted from the peels of *C. microcarpa* fruit collected in Dong Nai province, Vietnam, using steam distillation.

*Corresponding author.
Email address: lephamtanquoc@iuh.edu.vn
doi: 10.14456/easr.2025.50

2.2 Bacterial strains

This study utilized four bacterial strains, including the gram-positive species *Staphylococcus aureus* (ATCC 33591) and *Bacillus cereus* (ATCC 11778), and the gram-negative species *Escherichia coli* (ATCC 25922) and *Salmonella enteritidis* (ATCC 13076). These bacterial strains were provided by the Institute of Biotechnology and Food Technology, Ho Chi Minh City University of Industry.

2.3 Chemicals

The chemicals used in this study included 2,2-diphenyl-1-picrylhydrazyl (DPPH, purity ≥97%, Sigma, USA) and dimethyl sulfoxide (DMSO, purity ≥99.5%, GHTECH, China). Additionally, analytical-grade chemicals, culture media, and antimicrobial testing reagents such as nutrient broth and Mueller-Hinton agar (MHA; HiMedia, India), were used.

2.4 Preparation of CB-EO

CB-EO was synthesized based on the method described by Maleki et al. [6] with minor modifications. Initially, 4 g of chitosan was dissolved in 100 mL of 2% lactic acid solution at 55 °C with stirring at 600 rpm for 30 min. Subsequently, this mixture was blended with 0%, 0.5%, 1%, 1.5%, or 2% (v/v) CmEO, while also adding Tween 20 (0.2%, v/v). The sample without CmEO (0%, v/v) was used as a control. After stirring for 15 min, the resulting solution was dropped through a syringe into 50 mL of 2 M sodium hydroxide (NaOH) solution. The formed beads were washed five times with distilled water to remove residual NaOH from the surface, and then dried at 50 °C for 3 h. The CB-EO samples were collected, stored in sealed packaging at room temperature, and labeled according to the CmEO concentration: Control, CB-EO 0.5, CB-EO 1, CB-EO 1.5, and CB-EO 2. The entire chitosan bead production process is briefly illustrated in Figure 1.

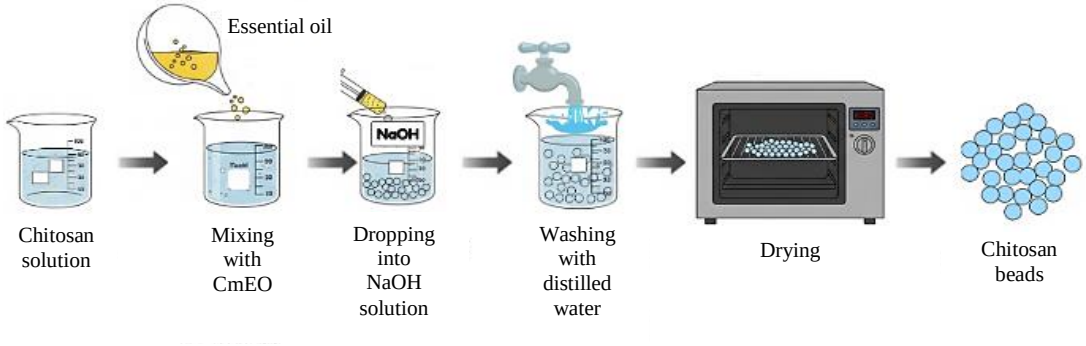

Figure 1 Flow diagram for the production of chitosan beads with *Citrus microcarpa* essential oil

2.5 Determination of bead collection efficiency

The bead collection efficiency was evaluated by determining the number of chitosan beads formed per unit volume of the initial polymer solution. Specifically, 10 mL of the prepared CB-EO mixture was loaded into a syringe and dropped into 2 M NaOH solution to induce bead formation. After complete gelation, the formed beads were collected, washed, and manually counted. The bead collection efficiency is expressed as the number of beads generated per 10 mL of the initial solution. This measure serves as an indicator of the performance and bead-forming capacity of each formulation under the given processing conditions.

2.6 Determination of bead size after drying

The length, width, and thickness of the beads were measured using a stainless steel digital caliper (Mitutoyo, model 500-182-30, USA). The equivalent diameter and sphericity of the beads were calculated using the formulas of Anam et al. [7]:

$$\text{Equivalent diameter} = (L \times W \times T)^{1/3} \text{ (mm)} \quad \text{(Eq. 1)}$$

$$\text{Sphericity} = \frac{ED}{L} \times 100 \text{ (\%)} \quad \text{(Eq. 2)}$$

where L, W, and T are the length, width, and thickness of the beads (mm), respectively.

2.7 Determination of the CB-EO swelling ratio

The swelling ratio of CB-EO beads was determined by using the gravimetric method of Farasat et al. [8], with appropriate modifications. Dry beads (0.2 g) were immersed in 10 mL of 0.9% sodium chloride (NaCl) for 30, 60, 90, or 120 min. Subsequently, the beads were drained and weighed to calculate the swelling ratio using the formula:

$$\text{Swelling ratio} = \frac{W_t}{W_0} \quad \text{(Eq. 3)}$$

where W_0 is the dry bead weight (g) and W_t is the wet bead weight (g).

2.8 Determination of CB-EO antioxidant activity

The antioxidant capacity of each CB-EO formulation was evaluated by assessing the DPPH radical scavenging activity, based on the procedure described by Sudharsan et al. [9] with some modifications. One gram of CB-EO was soaked in 15 mL of ethanol for 24 h. Then, 0.3 mL of the resulting solution was mixed with 2.7 mL of 0.1 mM DPPH solution and reacted for 30 min. The absorbance of the mixture was measured at 517 nm. The percentage of DPPH inhibition was calculated by using the formula:

$$\mathrm{DPPH_{RSC}}(\%) = \frac{A_0 - A_i}{A_0} \times 100 \quad \text{(Eq. 4)}$$

where A_0 represents the absorbance of the blank solution (DPPH solution) and A_i indicates the absorbance of the sample solution (DPPH solution and extract).

2.9 Determination of CB-EO antibacterial activity

The antibacterial activity of CB-EO was evaluated with the agar disc diffusion method according to Shi et al. [10], with appropriate modifications. Bacterial suspensions (0.1 mL, with a concentration of 1.5×10^8 colony-forming units (CFU)/mL, equivalent to 0.5 McFarland) were spread evenly on MHA in Petri dishes. CB-EO were placed on the agar surface along with the positive (gentamicin 10 µg/disc) and negative (5% DMSO) controls. The Petri dishes were incubated at 37 °C for 18 h, and then the diameter of the inhibition zone was measured.

2.10 FTIR spectroscopy

The FTIR spectra of the samples were recorded using a Tensor 27 spectrometer (Bruker Optik GmbH, Germany) in the wavenumber range from 4000 to 400 cm^{-1}, using a KBr beam splitter with a resolution of 1 cm^{-1}

2.11 XRD analysis

XRD analysis was performed on a AXS D8 Advance ECO X-ray diffractometer (Bruker). The measurements were conducted with a voltage of 40 kV and a current of 25 mA, and scanned in the 2θ angle range with a scanning rate of 0.2 rad/s.

2.12 Scanning electron microscopy (SEM) to assess surface morphology

The surface morphology of CB-EO was analyzed using a JSM-IT200 scanning electron microscope (JEOL, Japan) with a magnification of 30× and 2,000×, using an accelerating voltage of 5 kV. Before observation, the samples were naturally dried to remove surface moisture and then coated with a thin layer of platinum using a JEC-3000FC auto sputter coater (JEOL) to improve conductivity and image quality.

2.13 Data analysis

Each experiment was performed in triplicate, and the results are presented as the mean ± standard deviation. The STATGRAPHICS Centurion XV software was used for statistical analysis. One-way analysis of variance (ANOVA) was applied to determine differences between the groups, followed by the Tukey honestly significant difference test for pairwise comparisons with a significance level of 5%.

3. Results and discussion

3.1 Size of CB-EO

The addition of CmEO led to notable morphological changes to the chitosan beads. The bead length decreased from 1.70 to 1.43 mm as the EO concentration increased from 0% to 2% (v/v) (Table 1). This phenomenon can be attributed to the influence of CmEO on the chitosan gelation process, which limits the elongation of beads during formation, consistent with the findings reported by Bierhalz et al. [11].

The equivalent diameter, ranged from 1.39 to 1.54 mm, with no significant difference between the formulations. There may be alterations in the interactions between chitosan and CmEO that affect the shrinkage extent and the ability to maintain a bead shape [12].

The sphericity of CB-EO exhibited a notable improvement as the CmEO concentration increased, rising from 68.20% for the control to 89.30% for CB-EO 1.5. This suggests that CmEO contributes to the formation of more spherical and uniform beads by influencing chitosan shrinkage during bead formation. This phenomenon can be attributed to the intricate interactions between the hydrophobic components of CmEO and the hydrophilic chitosan polymer. Specifically, CmEO may modify the surface tension of the chitosan solution, thereby promoting the formation of more spherical droplets during the initial stages of bead formation by minimizing the surface energy [4]. These findings align with the research by Song et al. [13], who observed improved bead morphology with the incorporation of certain additives. These results are also consistent with the observations reported by Hosseini et al. [14], who described an increase in bead size as the EO concentration increased.

Overall, the addition of CmEO altered the bead size in terms of the length, width, and thickness, while also enhancing sphericity and affecting the equivalent diameter. These changes contribute to an improvement and enhancement of the material's properties.

Table 1 Size of chitosan beads with *Citrus microcarpa* essential oil (CB-EO)

Size	Control	CB-EO 0.5	CB-EO 1	CB-EO 1.5	CB-EO 2
Length (mm)	1.70^{b}±0.13	1.66^{b}±0.13	1.58^{ab}±0.25	1.46^{a}±0.07	1.43^{a}±0.15
Width (mm)	1.58^{b}±0.13	1.51^{b}±0.12	1.44^{b}±0.14	1.37^{ab}±0.21	1.21^{a}±0.22
Height (mm)	1.25^{a}±0.17	1.47^{b}±0.08	1.52^{b}±0.11	1.53^{b}±0.19	1.56^{b}±0.16
Equivalent diameter (mm)	1.49^{ab}±0.07	1.54^{b}±0.07	1.5^{b}±0.12	1.45^{ab}±0.11	1.39^{a}±0.08
Sphericity (%)	68.20^{a}±8.14	82.95^{ab}±5.73	86.65^{ab}±9.43	89.30^{ab}±8.62	87.59^{b}±8.50

Values in the same row with a different lowercase level are significantly different ($P < 0.05$).

3.2 Swelling ratio of CB-EO

Table 2 shows significant differences between the CB-EO samples regarding the water absorption capacity. The control sample exhibited the highest swelling ratio, ranging from 3.23 to 3.53. This indicates that chitosan beads possess a strong water absorption capacity due to their hydrophilic polymer structure, which facilitates the absorption and retention of water within the chitosan network [15]. Conversely, the CB-EO samples demonstrated a significantly lower swelling ratio, ranging from 1.10 to 2.57 times. This reduction can be attributed to the ability of CmEO to decrease the hydrophilicity of chitosan, thereby limiting its water absorption and swelling capacity. Additionally, CmEO may form hydrophobic interactions or enhance the mechanical strength of the beads, resulting in less expansion upon water exposure. This trend aligns with the findings of Abdollahi et al. [12], who reported that incorporating hydrophobic agents, such as EOs or plant extracts, into chitosan matrices reduces the number of available polar sites (e.g., –OH and –NH_2 groups) that can interact with water. As a result, the water affinity of the polymer network is reduced, contributing to decreased swelling behavior. This mechanism helps explain the reduced water uptake of the CB-EO samples.

In summary, the addition of CmEO significantly reduced the swelling ratio of chitosan beads. This could be advantageous in applications requiring materials with high durability and minimal deformation in aqueous environments.

Table 2 The swelling ratio of chitosan beads with *Citrus microcarpa* essential oil (CB-EO) over time

Time (min)	30	60	90	120
Control	3.23^{a}±0.18	3.53^{b}±0.08	3.50^{c}±0.1	3.30^{a}±0.13
CB-EO 0.5	1.10^{a}±0.11	1.08^{a}±0.06	1.27^{c}±0.19	1.15^{b}±0.13
CB-EO 1	2.55^{c}±0.08	2.37^{b}±0.20	2.57^{c}±0.15	2.17^{a}±0.08
CB-EO 1.5	1.09^{b}±0.08	1.15^{d}±0.05	1.05^{a}±0.05	1.12^{c}±0.03
CB-EO 2	1.35^{a}±0.06	1.68^{c}±0.1	1.57^{b}±0.16	1.72^{d}±0.13

Values in the same row with a different lowercase level are significantly different ($P < 0.05$).

3.3 Bead formation efficiency

As shown in Table 3, the number of beads collected in 10 mL of solution increased with the CmEO concentrations. Specifically, the control sample had the lowest number of beads (177 beads), while CB-EO 1.5 had the highest number (263 beads). This increase may be related to the size changes observed in Table 1, particularly the trend of decreasing length and equivalent diameter as the CmEO concentration increased, resulting in smaller but more numerous beads. To date, no studies have evaluated bead collection efficiency, so there is nothing to which the results of this study can be compared.

Table 3 Particle formation efficiency of chitosan beads with *Citrus microcarpa* essential oil (CB-EO) per 10 mL of solution

Yield	Control	CB-EO 0.5	CB-EO 1	CB-EO 1.5	CB-EO 2
Number of beads per 10 mL	177^{a}±3	228^{b}±2	234^{c}±4	263^{e}±3	243^{d}±3

Values in the same row with a different lowercase level are significantly different ($P < 0.05$).

3.4 Antioxidant activity of CB-EO

As shown in Table 4, the antioxidant capacity of the chitosan beads improved significantly with the addition of CmEO, with a trend for increasing activity as the CmEO concentration increased. The control sample still exhibited 9.69% DPPH radical scavenging activity, indicating that chitosan itself possesses a certain level of antioxidant activity. However, upon the addition of EO, this activity increased significantly, from 24.17% (for CB-EO 0.5) to 77.96% (for CB-EO 2), which is 8 times higher than the control sample. This trend is consistent with the research by Su et al. [16], who also reported an increase in antioxidant activity as the EO concentration increased.

This improvement is attributed to the presence of polyphenols and bioactive compounds in CmEO, which enhance the ability to neutralize free radicals. This also confirms that the combination of chitosan and CmEO creates a synergistic effect, enhancing the antioxidant properties of the beads [17]. Furthermore, this antioxidant activity may manifest through the ability to maintain the stability of the biomaterial, extending the shelf life of food products. This antioxidant capacity opens up potential application avenues.

Table 4 Antioxidant activity of chitosan beads with *Citrus microcarpa* essential oil (CB-EO)

Antioxidant activity	Control	CB-EO 0.5	CB-EO 1	CB-EO 1.5	CB-EO 2
$DPPH_{RSC}$ (%)	9.69^{a}±1.97	24.17^{b}±1.53	49.59^{c}±0.96	64.54^{d}±0.64	77.96^{e}±0.76

Values in the same row with a different lowercase level are significantly different ($P < 0.05$).

3.5 Antibacterial activity of CB-EO

Table 5 shows that the control sample exhibited antibacterial activity, with an inhibition zone diameter ranging from 2.04 mm (*S. aureus*) to 3.15 mm (*S. enteritidis*). This confirms the inherent antibacterial activity of chitosan, which can be attributed to its cationic nature—it disrupts bacterial cell membranes [18]. Similarly to the antioxidant capacity, the addition of CmEO enhanced antibacterial activity compared with the control. CB-EO 1.5 and CB-EO 2, with the highest CmEO concentrations, presented the highest antibacterial activity. However, compared with the positive control (gentamicin), the CB-EO samples presented significantly lower antibacterial activity. Overall, gentamicin exhibited the strongest antibacterial effect against all four bacterial species. Specifically, they presented an inhibition zone diameter ranging from 16.57 to 24.19 mm. Notably, the inhibition zone diameter of the CB-EO 0.5 to CB-EO 2 samples showed significant variation (from 2.7 to 9.44 mm), possibly due to the influence of the bead size, the CmEO release rate, and the diffusion capacity within the culture medium. This aligns with the research by Junca et al. [4], who indicated that chitosan acts as a reservoir for EOs, slowing down evaporation and thus prolonging storage time.

Table 5 Antibacterial activity of chitosan beads with *Citrus microcarpa* essential oil (CB-EO)

Strains	Control	CB-EO 0.5	CB-EO 1	CB-EO 1.5	CB-EO 2	Gentamicin
S. enteritidis	3.15^{a}±0.05	7.0^{b}±0.68	5.88^{b}±0.15	9.44^{c}±0.05	6.21^{b}±0.07	21.22^{d}±1.13
B. cereus	2.45^{a}±0.01	7.26^{c}±0.02	3.16^{b}±0.02	8.31^{e}±0.03	6.24^{b}±0.04	24.19^{f}±0.41
E. coli	2.33^{a}±0.03	5.68^{d}±0.02	3.14^{b}±0.03	7.89^{e}±0.03	5.26^{c}±0.02	18.90^{f}±0.11
S. aureus	2.04^{a}±0.04	4.43^{c}±0.02	2.70^{b}±0.03	7.21^{e}±0.02	6.25^{d}±0.02	16.57^{f}±0.03

Values in the same row with a different lowercase level are significantly different ($P < 0.05$).

The growth of all tested bacterial strains was inhibited because the EO penetrates the lipid layer of the cell membrane and alters their structure, making them more porous. Consequently, ions and other cellular components leak through the membrane, potentially leading to cell death. Additionally, phenolic compounds can alter membrane permeability and subsequently the rate of penetration into bacterial cells, causing loss of integrity and, again, cell death [19].

3.6 FTIR spectroscopy of CB-EO

The FTIR spectra clearly reflect the interaction between chitosan and CmEO at the tested concentrations (Figure 2). Upon the addition of CmEO, the absorption peak at ~3300 cm^{-1} (–OH stretching) tended to shift and decrease in intensity, indicating the formation of hydrogen bonds between CmEO and chitosan. Additionally, the band at ~1650 cm^{-1} (C=O of amide) was reduced, suggesting that CmEO may have interacted with the amino groups ($–NH_2$) in chitosan, altering the polymer structure [20]. Notably, as the CmEO concentration increased, several new peaks appeared in the range of 2900–2950 cm^{-1}, possibly due to C–H bond vibrations in the CmEO components. Simultaneously, some characteristic chitosan peaks in the 1000–1200 cm^{-1} region (C-O-C stretching) decreased in intensity or disappeared, indicating changes in the polymer network structure. It can be inferred that chitosan molecules established intramolecular and intermolecular hydrogen bonds through their –OH and –NH functional groups with the –OH groups of the most common components in CmEO, as proposed in the study by Bajić et al. [21]. These changes are similar to previous studies on chitosan biopolymer films upon the addition of plant extracts, suggesting a reorganization of bonds within the material [22].

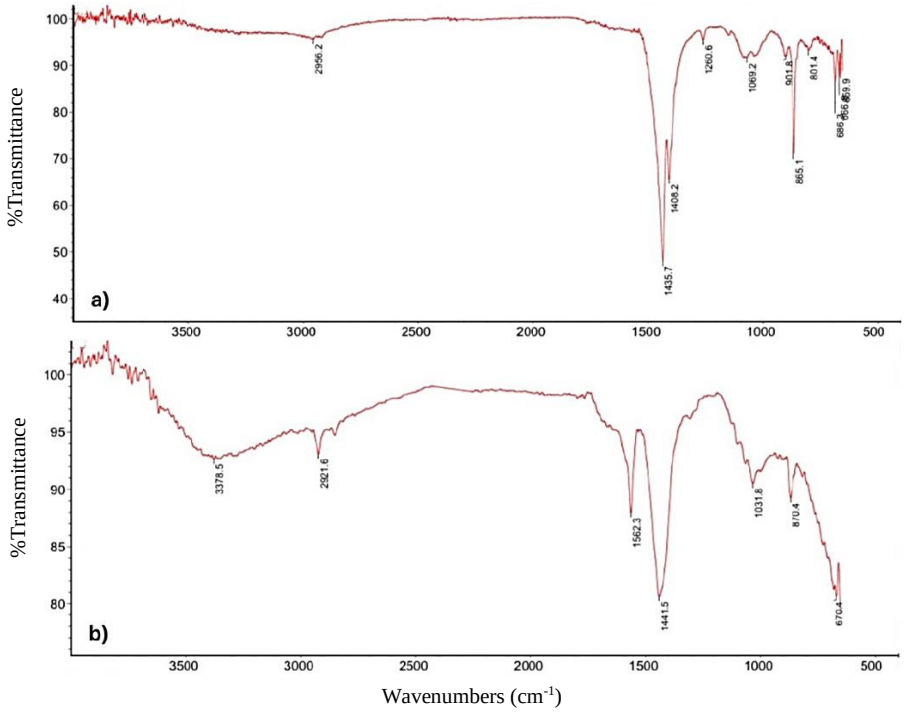

Figure 2 Fourier-transform infrared spectra of chitosan beads with *Citrus microcarpa* essential oil (CB-EO): (a) CB-EO 2, (b) CB-EO 1.5, (c) CB-EO 1, (d) CB-EO 0.5, and (e) control

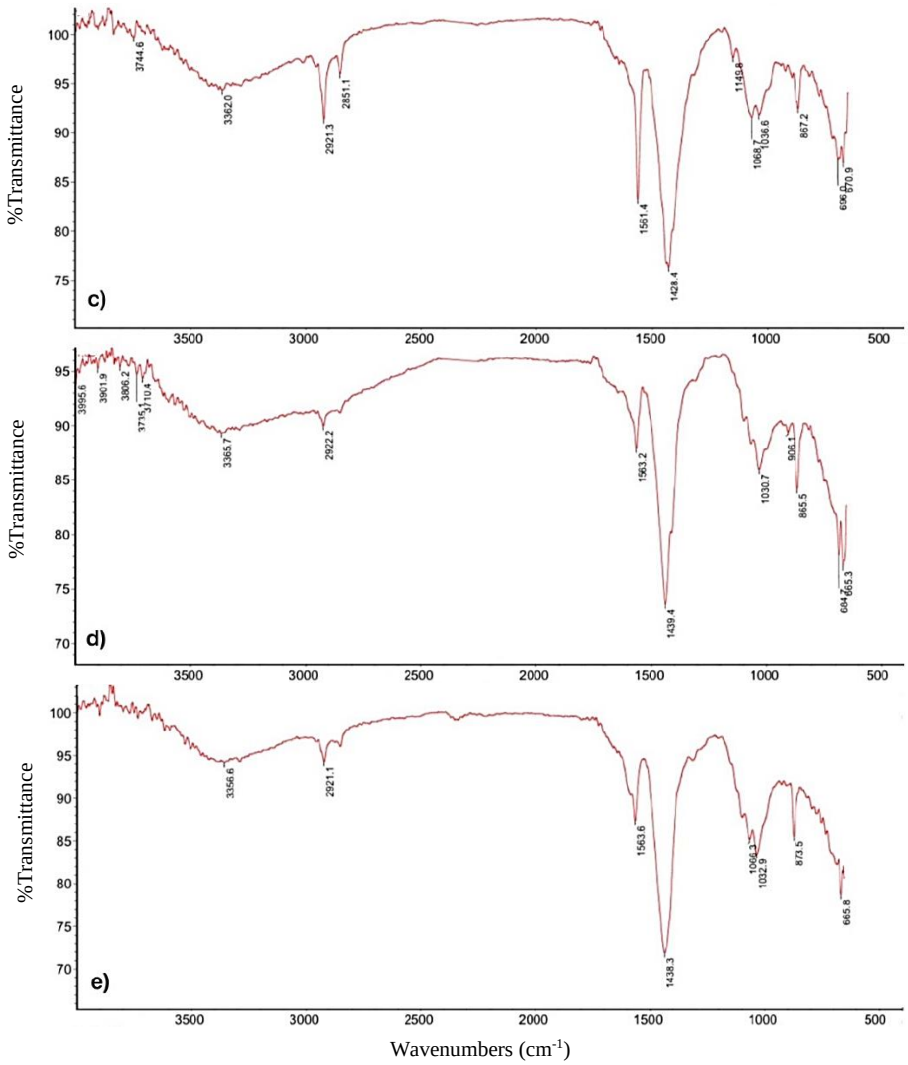

Figure 2 (continued) Fourier-transform infrared spectra of chitosan beads with *Citrus microcarpa* essential oil (CB-EO): (a) CB-EO 2, (b) CB-EO 1.5, (c) CB-EO 1, (d) CB-EO 0.5, and (e) control

3.7 SEM analysis of CB-EO

Figure 3 presents scanning electron micrographs of CB-EO samples at 30× and 2000×. At low magnification (30×), the micrographs show the overall shape and distribution of the chitosan beads. The beads tended to maintain a spherical shape and uniform distribution; however, surface cracks and small pores began to appear as the CmEO concentration increased from 0.5% to 2% (v/v). At high magnification (2000×), the surface details are clearer, revealing a significant increase in roughness and the number of larger cracks and pores as the CmEO concentration increased. In particular, CB-EO 1.5 and CB-E0 2 showed very rough surfaces with numerous large cracks and pores, reflecting the strong influence of CmEO on the microstructure of the beads. This trend is consistent with the report by Atarés and Chiralt [23], who reported that the addition of EO to biopolymer films reduces uniformity and increases surface roughness.

These changes can affect the physical and chemical properties of the beads, including release capacity, mechanical strength, and interaction with the surrounding environment. These changes are useful for the design and application of chitosan beads in fields such as biomedicine, food, and cosmetics.

3.8 XRD analysis of CB-EO

The XRD patterns revealed a clear change in the crystalline structure of chitosan upon incorporation of CmEO. Pure chitosan exhibited characteristic peaks at approximately 10° and 20° (2θ), reflecting its semi-crystalline structure [24]. However, with the addition of CmEO, these peaks became broader and decreased in intensity, indicating a reduction in crystallinity (Figure 4). This may be attributed to disruption of the ordered arrangement of chitosan polymer chains by CmEO, leading to an increase in amorphousness [25]. At the two highest CmEO concentrations (1.5% and 2%, v/v), new peaks appeared in the range of 15–25° (2θ), which may be related to the formation of new crystalline phases due to interactions between CmEO and the chitosan network. The increase in amorphousness can improve the solubility and active ingredient release of chitosan, while also affecting mechanical properties such as strength and elasticity [26]. The XRD results are consistent with previous studies, demonstrating that EOs can significantly alter the structure and properties of chitosan.

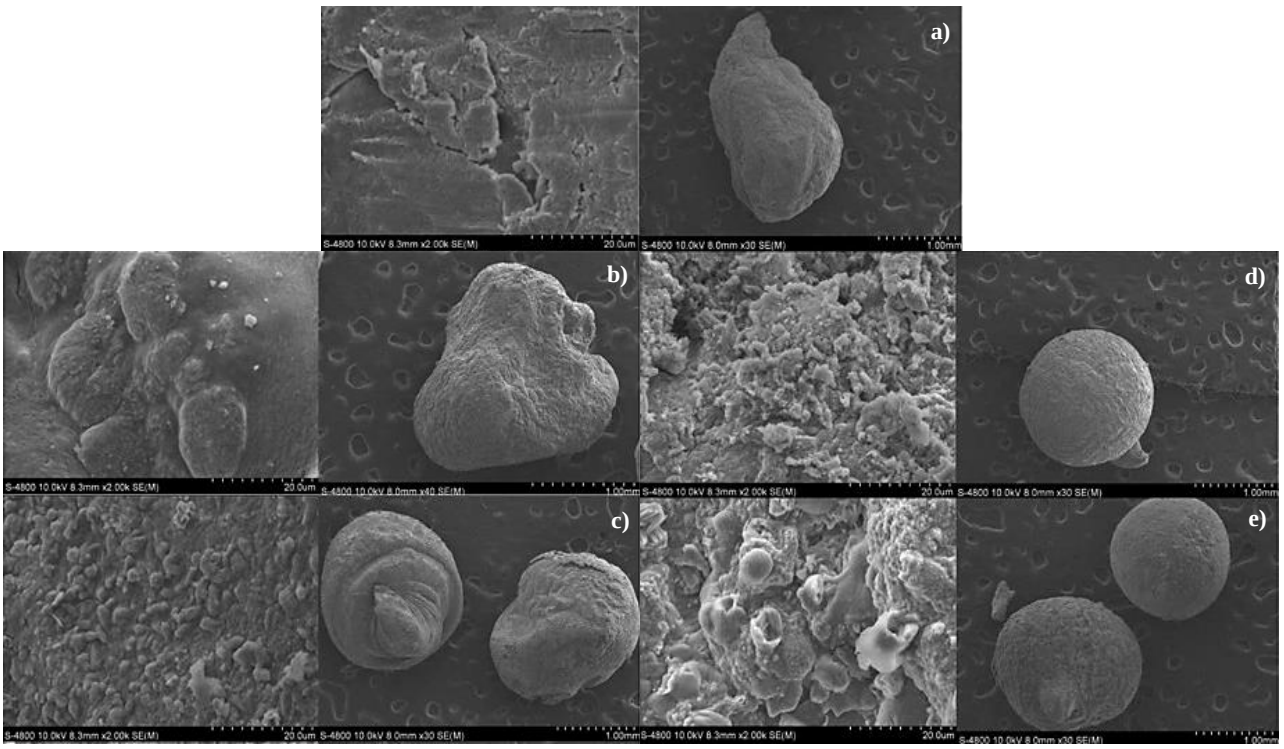

Figure 3 Scanning electron micrographs of chitosan beads with *Citrus microcarpa* essential oil (CB-EO) at 2000× (left) and 30× (right) magnification: (a) control, (b) CB-EO 0.5, (c) CB-EO 1, (d) CB-EO 1.5, and (e) CB-EO 2.

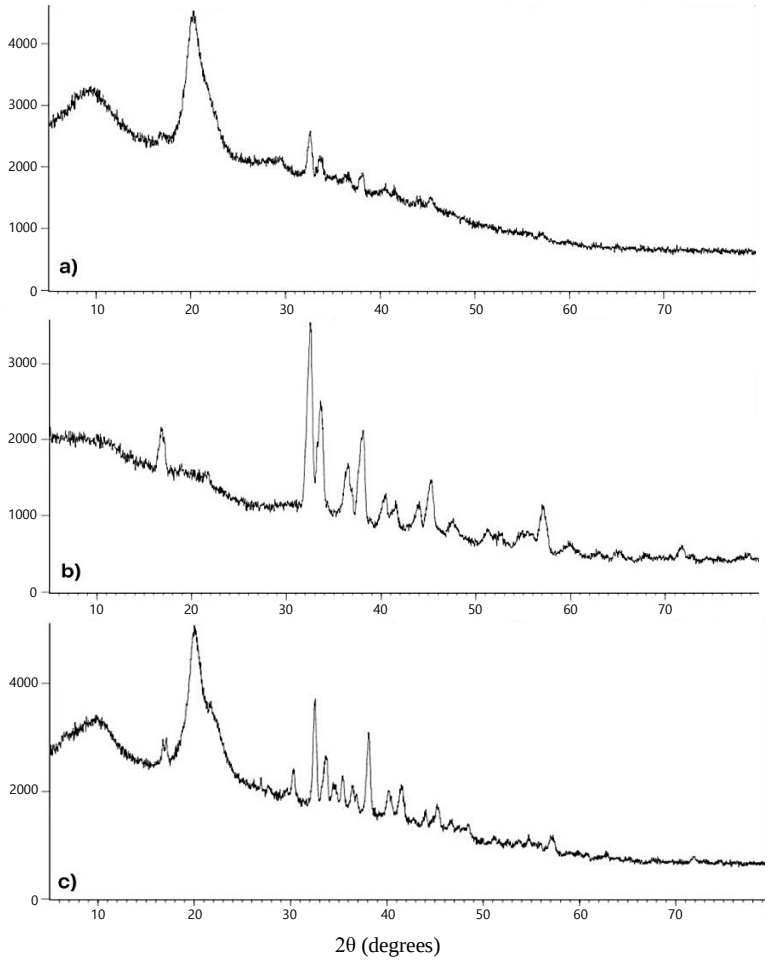

Figure 4 X-ray diffraction analysis of chitosan beads with *Citrus microcarpa* essential oil (CB-EO): (a) CB-EO 2, b) CB-EO 1.5, (c) CB-EO 1, (d) CB-EO 0.5, and (e) control

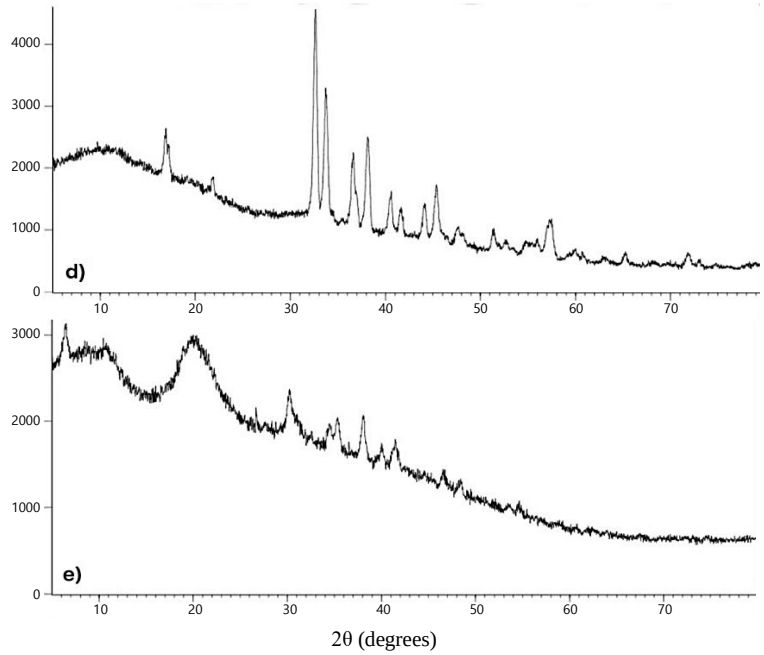

Figure 4 (continued) X-ray diffraction analysis of chitosan beads with *Citrus microcarpa* essential oil (CB-EO): (a) CB-EO 2, b) CB-EO 1.5, (c) CB-EO 1, (d) CB-EO 0.5, and (e) control

In general, a higher CmEO content led to a smaller bead size and a lower swelling ratio, which could be attributed to the hydrophobic nature of CmEO reducing water uptake and limiting bead expansion. The bead formation efficiency varied among the samples: As the CmEO concentration increases, a larger number of more compact beads was produced, likely due to the influence of viscosity and emulsion stability during dripping. FTIR spectroscopy revealed stronger molecular interactions between CmEO and chitosan, particularly in CB-EO 1.5 and CB-EO 2, as evidenced by shifts and intensity changes in characteristic bands. These interactions may contribute to the reduce the swelling capacity and increase mechanical integrity. The SEM observations supported these findings, showing more compact surface morphology and better sphericity in CB-EO, especially with higher CmEO concentrations. Meanwhile, XRD patterns indicated decreased crystallinity in the CB-EO samples, reflecting the structural changes caused by CmEO incorporation. Taken together, the combination of reduced swelling, altered morphology, and lower crystallinity suggests that CmEO not only modifies the internal structure but also improves the functional stability of chitosan beads.

4. Conclusion

This study investigated the potential of incorporating CmEO into chitosan beads for sustainable food packaging. The results demonstrated a significant enhancement in both antioxidant and antibacterial properties of chitosan upon CmEO addition. Notably, CB-EO 2, with the highest CmEO concentration, exhibited remarkable DPPH radical scavenging activity of 77.96%. Antibacterial assays further confirmed the efficacy of CmEO, showing inhibitory effects against common foodborne pathogens, including *E. coli*, *B. cereus*, *S. enteritidis*, and *S. aureus*. Moreover, the addition of CmEO altered the performance, size, and crystallinity of chitosan beads, highlighting its influence on the physicochemical properties of the material. These results validate the potential of using CmEO-loaded chitosan beads as an environmentally friendly alternative to synthetic materials. For future development, the system could be modified for active food packaging, edible coatings, or controlled-release applications. Further research is advised to assess long-term storage stability, release mechanisms in real food systems, and regulatory factors for commercial use.

5. References

[1] Panou G, Karabagias IK. Biodegradable packaging materials for foods preservation: sources, advantages, limitations, and future perspectives. Coatings. 2023;13(7):1176.
[2] Wang X, Xue Z, Sun Y, Peng B, Wu C, Kou X. Chitosan-ginger essential oil nanoemulsions loaded gelatin films: a biodegradable material for food preservation. Int J Biol Macromol. 2024;280:135791.
[3] Perdones A, Sánchez-González L, Chiralt A, Vargas M. Effect of chitosan–lemon essential oil coatings on storage-keeping quality of strawberry. Postharvest Biol Technol. 2012;70:32-41.
[4] Junca MAV, Valencia C, Flórez López E, Delgado-Ospina J, Zapata PA, Solano M, et al. Chitosan beads incorporated with essential oil of *Thymus capitatus*: stability studies on red Tilapia fillets. Biomolecules. 2019;9(9):458.
[5] Tsai PW, Roxas TJR, Tayo LL, Lin YR, Hsueh CC, Chen BY. Unveiling bioenergy-stimulating and electron-transporting characteristics of metabolites from *Citrus microcarpa* peels and pulps as medicated diet of sustainable energy resource. Biochem Eng J. 2023;196:108951.
[6] Maleki G, Woltering EJ, Mozafari MR. Applications of chitosan-based carrier as an encapsulating agent in food industry. Trends Food Sci Technol. 2022;120:88-99.
[7] Anam A, Haryanto F, Widita R, Arif I, Dougherty G. Automated calculation of water-equivalent diameter (DW) based on AAPM task group 220. J Appl Clin Med Phys. 2016;17(4):320-33.
[8] Farasat F, Sefti MV, Sadeghnejad S, Saghafi HR. Effects of reservoir temperature and water salinity on the swelling ratio performance of enhanced preformed particle gels. Korean J Chem Eng. 2017;34:1509-16.

[9] Sudharsan S, Velpandian V, Kumar MP, Banumathi V. Evaluation of antioxidant activity of *Nilapanai kizhangu chooranam* through DPPH scavenging assay. Int J Adv Res Biol Sci. 2017;4(2):28-31.
[10] Shi LW, Zhuang QQ, Wang TQ, Jiang XD, Liu Y, Deng JW, et al. Synthetic antibacterial quaternary phosphorus salts promote methicillin-resistant *Staphylococcus aureu*s-infected wound healing. Int J Nanomedicine. 2023;18:1145-58.
[11] Bierhalz ACK, da Silva MA, Kieckbusch TG. Natamycin release from alginate/pectin films for food packaging applications. J Food Eng. 2012;110(1):18-25.
[12] Abdollahi M, Rezaei M, Farzi G. Improvement of active chitosan film properties with rosemary essential oil for food packaging. Int J Food Sci Technol. 2012;47(4):847-53.
[13] Song G, Sun R, Li H, Zhang H, Xia N, Guo P, et al. Effects of pine needle essential oil combined with chitosan shellac on physical and antibacterial properties of emulsions for egg preservation. Food Biophysics. 2022;17(2):260-72.
[14] Hosseini MH, Razavi SH, Mousavi MA. Antimicrobial, physical and mechanical properties of chitosan-based films incorporated with thyme, clove and cinnamon essential oils. J Food Process Preserv. 2009;33(6):727-43.
[15] Kavoosi G, Rahmatollahi A, Dadfar SMM, Purfard AM. Effects of essential oil on the water binding capacity, physico-mechanical properties, antioxidant and antibacterial activity of gelatin films. LWT-Food Sci Technol. 2014;57(2):556-61.
[16] Su H, Huang C, Liu Y, Kong S, Wang J, Huang H, et al. Preparation and characterization of cinnamomum essential oil–chitosan nanocomposites: physical, structural, and antioxidant activities. Processes. 2020;8(7):834.
[17] Ghahfarokhi MG, Barzegar M, Sahari MA, Azizi MH. Enhancement of thermal stability and antioxidant activity of thyme essential oil by encapsulation in chitosan nanoparticles. J Agric Sci Technol. 2016;18:1781-92.
[18] Aider M. Chitosan application for active bio-based films production and potential in the food industry. LWT-Food Sci Technol. 2010;43(6):837-42.
[19] Lin CM, Preston JF 3rd, Wei CI. Antibacterial mechanism of allyl isothiocyanate. J Food Prot. 2000;63(6):727-34.
[20] Siripatrawan U, Vitchayakitti W. Improving functional properties of chitosan films as active food packaging by incorporating with propolis. Food Hydrocoll. 2016;61:695-702.
[21] Bajić M, Ročnik T, Oberlintner A, Scognamiglio F, Novak U, Likozar B. Natural plant extracts as active components in chitosan-based films: a comparative study. Food Packag Shelf Life. 2019;21:100365.
[22] Gradinaru LM, Barbalata-Mandru M, Enache AA, Rimbu CM, Badea GI, Aflori M. Chitosan membranes containing plant extracts: preparation, characterization and antimicrobial properties. Int J Mol Sci. 2023;24(10):8673.
[23] Atarés L, Chiralt A. Essential oils as additives in biodegradable films and coatings for active food packaging. Trends Food Sci Technol. 2016;48:51-62.
[24] Kumar S, Koh J. Physiochemical, optical and biological activity of chitosan-chromone derivative for biomedical applications. Int J Mol Sci. 2012;13(5):6102-16.
[25] Ahari H, Kalateh-Seifari F, Yousefi S. Antimicrobial activity of chitosan/corn starch film incorporated with starch nanocrystals/nettle essential oil nanoemulsion for *Eleutheronema tetradactylum* fillet preservation. Food Chem X. 2025; 25:102085.
[26] Shete A, Chavan A, Potekar P, Yadav G, Shah N. Modification of physicochemical properties of chitosan to improve its pharmaceutical and agrochemical potential applications. Int J Biol Macromol. 2024;267:131404.